Analyst

Accepted Manuscript

This article can be cited before page numbers have been issued, to do this please use: L. Liu , L. Zhang, Z. Dai and Y. Tian, *Analyst*, 2017, DOI: 10.1039/C7AN00138J.

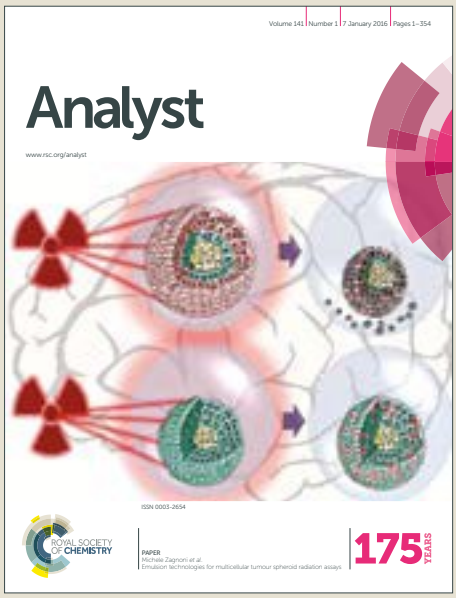

ROYAL SOCIETY OF CHEMISTRY

rsc.li/analyst

View Article Online
DOI: 10.1039/C7AN00138J

Journal Name

ARTICLE

Facile Functional Carbon Nanotube Fiber for In Vivo Monitoring NO in a Rat Brain Followed by Cerebral Ischemia

Received 00th January 20xx,
Accepted 00th January 20xx

DOI: 10.1039/x0xx00000x

www.rsc.org/

Li Liu,[a,b] Limin Zhang,*,[b] Zhihui Dai,*,[a] Yang Tian[b]

NO is key free-radical messenger and neuronal signal which is closely related to many brain diseases. It is a challenge to develop a sensitive and reliable biosensor for in vivo monitoring NO in brain. Here, a facile ratiometric electrochemical biosensor for NO monitoring in rat brain followed by cerebral ischemia was developed on the basis of carbon nanotube fiber (CNF) modified by hemin, in which CNF not only served as a platform to assemble hemin molecule, but greatly facilitated the electron transfer of hemin on the electrode surface. Additionally, hemin molecule played dual roles: a stable catalyst for reduction of NO toward selective detection of NO at -0.67 V vs. Ag/AgCl, as well as an inner reference element to provide a built-in correction, avoiding the interference from complicated brain environment. The developed ratiometric biosensor can detect NO with a linear range from 25 to 1000 nM, with a low limit of detection down to 10 nM, which fulfills the requirements for in vivo measurement of NO. The remarkable analytical performance of the *present* biosensor, as well as the long-term stability and good reproducibility established a reliable approach for in vivo monitoring NO in hippocampus of rat brains followed by cerebral ischemia. It was first report that the average level of NO increased from 61 ± 23 nM to 141 ± 18 nM after cerebral ischemia for 15 min.

Introduction

Nitric oxide (NO) is a key free-radical messenger involved in a wide range of physiological and pathological processes.[1, 2] In the brain, NO regulates vascular tone, acts as a neuronal signal in the gastrointestinal tract and central nervous system, and contributes to the pathology of several brains diseases including ischemia, Parkinson's disease and Alzheimer's disease. The main blockade for NO in vivo measurement includes the low concentration in brain of sub-micromolar, short half-life within 1 min in tissue,[3, 4] and high affinity for interaction with O_2, peroxides and the superoxide anion ($O_2^{\bullet-}$). Thus, development of monitoring strategies for NO in vivo with good selectivity, sensitivity and fast response are essential to progress our understanding of the roles of NO playing in pathological and physiological events in the brain and related brain diseases.[5, 6]

Up to now, the majority of analytical approaches for measuring NO includes chemiluminescence, Raman spectra, EPR spectroscopy, fluorescence, and electrochemical methods.[7-14] However, most spectroscopic methods present obstacle for in vivo NO detection due to the complex instrumentation that is difficult to miniaturize.[15, 16] In contrast, electrochemical methods show remarkably advantages in their speed, easy miniaturation, real-time measurement, and in vivo determination.[17-25] In those investigations, the material used to construct an electrochemical NO sensor plays a pivotal role in the sensitivity and stability.[26-28] However, the involvement of manual modification procedures through coating nanomaterials on the electrode surface might increase the risk of person-to-person or electrode-to-electrode deviation during the measurement.[29, 30] Such situation would become more serious in complicate biological system, like in brain. In addition, the other question for in vivo measurement of NO is that most biosensors of NO suffer from significant baseline drift when employed directly in biological sample, particularly in brain, mainly due to the bio-fouling of electrode from protein, peptide, and cell.[31] Thus, it is still a challenging work to develop a more facile, reliable and accurate electrochemical biosensor for determination of NO in a rat brain.

In the present work, we established a new approach to detect NO in vivo using a novel CNT fiber modified by hemin (Fig. 1). The CNF was demonstrated to possess uniformed surface structure and small diameter of ~10 μm. Furthermore, the CNF comprising of abundant carbon nanotubes, provided a high surface-to-volume ratio, and greatly enhanced the direct electron transfer of hemin assembled on the electrode surface. Such integration of microelectrode with nanomaterials not only simplifies the electrode fabrication procedure, but also greatly improves the sensitivity and

[a] Jiangsu Collaborative Innovation Centre of Biomedical Functional Materials and Jiangsu Key Laboratory of Biofunctional Materials, School of Chemistry and Materials Science, Nanjing Normal University, Nanjing 210023 (P. R. China)
[b] Shanghai Key Laboratory of Green Chemistry and Chemical Processes, Department of Chemistry, School of Chemistry and Molecular Engineering, East China Normal University, Dongchuan Road 500, Shanghai 200241, China.
† Footnotes relating to the title and/or authors should appear here.
Electronic Supplementary Information (ESI) available: [details of any supplementary information available should be included here]. See DOI: 10.1039/x0xx00000x

View Article Online
DOI: 10.1039/C7AN00138J

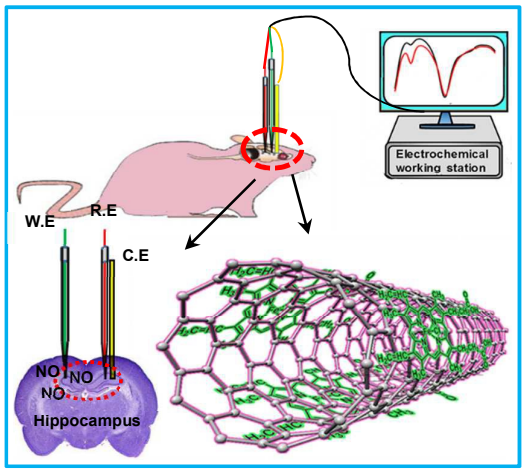

Fig. 1. Developed ratiometric electrochemical sensor for real-time monitoring of NO in a rat brain followed by global cerebral ischemia.

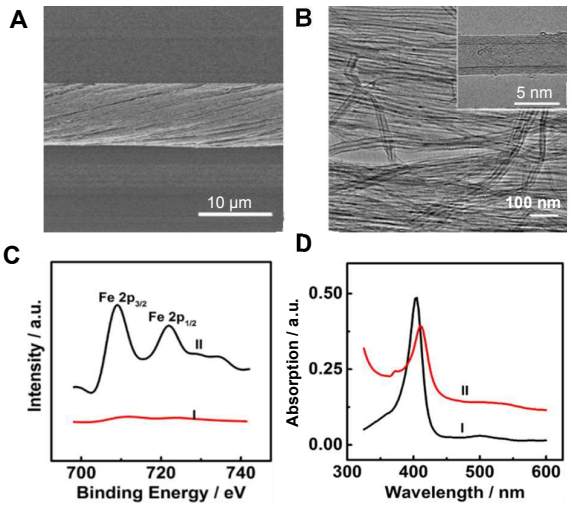

Fig. 2. (A) SEM image of CNF; (B) TEM image of MWCNTs for CNF. Inset: TEM image of a single MWCNT. (C) XPS spectra of Fe 2p at CNF (I) and CNF/hemin (II); (D) UV-Vis spectra obtained in DMSO solution of 10 mM hemin (I) and suspension of 10 mM hemin with CNFs (II).

reproducibility of electrode.[32, 33] On the other hand, hemin with good stability was modified on the CNF. The hemin immobilized on the electrode surface was expected to have dual roles, a catalyst for reduction of NO [34, 35] toward the selective detection of NO at -0.67 V vs. Ag/AgCl, and an inner reference element to provide a built-in correction, avoiding the interferences from complicated brain environment and leading to ratiometric determination with high accuracy. Then, Nafion was covered as a bio-fouling layer to defend the interference from anions and macromolecules. Finally, combined with unique properties of CNF including easy to insert in the live brain and good biocompatibility, the developed biosensor succeeded in directly evaluating the levels of NO in a live rat brain. The concentration of NO increased by 1.3-fold in hippocampus of rat brain upon cerebral ischemia, compared with those in the normal rat brain.

Results and discussion

Characterization of hemin-modified CNF microelectrode.

Motivated by development of NO biosensor available for in vivo determination in the complicate rat brain with high sensitivity and reliability, CNF was dry-spun from multi-walled carbon nanotube (MWCNT) arrays with revolving speed of about 2000 rpm.[36] As shown in Fig. 2A, a CNF composes of carbon nanotube (CNT) bundles with a uniform diameter of ~ 10 μm. The abundant CNTs in CNF showed smooth multi-walled structure with averaged diameter of ~5 nm (Fig. 2B). The modification of hemin was verified by XPS. As demonstrated in Fig. 2C (Curve II), two obvious peaks located at 708 eV for Fe $2p_{3/2}$, and 723 eV for Fe $2p_{3/2}$ were observed clearly after modification of hemin, while no peak was obtained at bare CNF electrode (Fig. 2C, Curve I), suggesting hemin has been successfully assembled on the CNF surface.

Then, UV-Vis spectroscopy was further employed to demonstrate the non-covalent binding of hemin molecule on electrode surface. As shown in Fig. 2D (Curve I), a strong absorption peak at ~ 387 nm was observed in hemin solution. But the absorption peak moved to 398 nm in mixed suspension of hemin and CNFs (Curve II in Fig. 2D). The bathochromic shift of ~11 nm in the absorption peak suggests that π–π interaction between hemin molecule and CN.[37]

Electrochemical responses of the CNF/hemin/Nafion microelectrode

Differential pulse voltammetry (DPV) was employed for electrochemical measurements of NO because of its high sensitivity. Fig. 3A shows DPV signals obtained at (I) bare CNF, (II) CNF/hemin, and (III) CNF/hemin/Nafion electrodes in aCSF (pH 7.4). A clear cathodic peak located at -0.33 V vs Ag/AgCl was observed at the CNF/hemin electrode in aCSF (pH 7.4) (Fig. 3A, Curve II), while no obvious response was obtained at bare CNF electrode (Fig. 3A, Curve I). Such cathodic peak at -0.33 V was attributed to the reduction process of $Fe^{3+/2+}$, electroactive center in hemin molecule, confined on CNF electrode surface through strong π-π stacking interaction. Then, Nafion was covered on the CNF/hemin microelectrode to protect the electrode from the interference of anions and biofouling from macromolecules, and cells in brain. Negligible change for hemin electrochemical response was observed (Fig. 3A, Curve III), indicating that coating of Nafion would not block the electron transfer of hemin molecule at the CNF microelectrode surface. From the relationship between anodic and cathodic peak currents of hemin and potential scan rates, we found that the redox process of hemin molecules on the

View Article Online
DOI: 10.1039/C7AN00138J

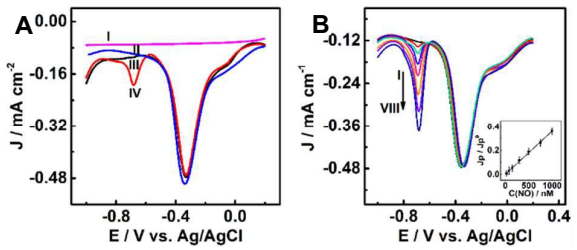

Fig. 3. (A) DPV responses obtained in N_2-saturated aCSF (pH 7.4) at (I) bare CNF, (II) hemin/CNF, (III) CNF/hemin/Nafion microelectrodes in the absence and (IV) presence of 150 nM NO. (B) DPV obtained at CNF/hemin/Nafion microelectrode in aCSF (pH 7.4) contained 50 μM O_2 with different concentrations of NO, they are (I) 0 nM; (II) 25 nM; (III) 80 nM; (IV) 150 nM; (V) 300 nM; (VI) 500 nM; (VII) 750 nM; (VIII) 1000 nM, respectively. Inset: The calibration plot of J_p/J_p^0 against concentration of NO.

electrode surface was the surface-confined process (Fig. S1, SI). The rate constant of the heterogeneous electron transfer (Ks) of hemin on CNF microelectrode was estimated to be ~11.98 s^{-1}, which is much greater than that obtained at metal electrode modified by hemin (~ 0.67 s^{-1}),[38, 39] suggesting that the electron transfer of hemin was greatly facilitated on the developed CNF electrode surface. Such large Ks might originate from the cleaner and more defects of MWCNT in CNF produced after heating treatment (Fig. S2, SI) than that of raw MWCNT. With the addition of NO into aCSF (pH 7.4), a new cathodic peak appeared at -0.67 V vs Ag/AgCl, which was ascribed to the reduction of NO catalyzed by hemin on the electrode surface (Fig. 3A, Curve IV). The electrocatalytic reduction of NO by hemin can be elucidated by the following reactions mechanism: [40]

Fe (II) + NO ⟶ Fe (II)–NO
Fe (II)–NO + H^++e- ⟶ Fe (II)–HNO
Fe (II)–HNO + $2H^+$+ $2e^-$ ⟶ Fe (II) + H_2NOH

Furthermore, the cathodic peak current density (J_p) observed at -0.67 V gradually increased with increasing concentrations of NO, while that of hemin at -0.33 V (J_p^0) kept almost constant (as shown in Fig. 3B), resulting in the ratiometric determination of NO with high accuracy. Moreover, the ratiometric peak current density ratio (J_p/J_p^0) exhibited a good linearity with the concentration of NO in the range of 20 to 1000 nM with a detection limit down to ~ 10 nM (S/N = 3:1) (Fig. 3B, inset). The electrochemical signals for hemin at CNF/hemin were estimated to be ~10-fold greater than that obtained at carbon fiber modified by hemin, owing to the large surface area and electrocatalytic activity of CNF (Fig S3, SI). More importantly, the CNF/hemin/Nafion electrode exhibited fast response time for NO within 1 min (Fig. S4, SI). The current CNF/hemin/Nafion microsensor demonstrated a wider linear range, higher sensitivity, and relatively low detection limit, compared with the previous electrochemical sensors of NO (Table S1).

The complexity of the brain system presents a great challenge to selective detection of NO. Here, the selectivity of CNF/hemin/Nafion electrode for NO was evaluated by monitoring J/J_{NO} induced by potential interfering species (J represents J_p/J_p^0 value for various interferences) against that of NO (J_{NO} is J_p/J_p^0 value for 500 nM NO) (Fig. 4). The potential

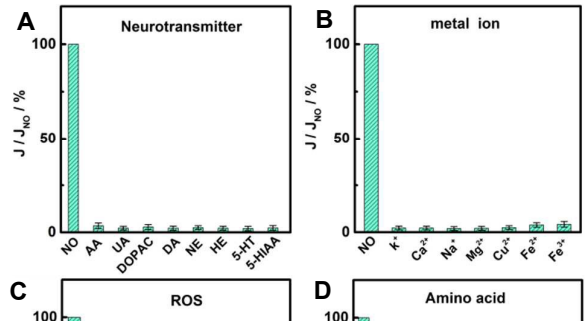

Fig. 4. (A) Selectivity tests for neurotransmitters against NO (1) 500 nM NO; (2) 400 μM AA; (3) 10 μM UA; (4) 10 μM DOPAC; (5) 10 μM DA; (6) 10 μM 5-HT; (7)10 μM 5-HIAA. (B) Selectivity tests for metal ions against NO (1) 500 nM NO; (2) 1 mM K^+; (3) 10 μM Ca^{2+}; (4) 1 mM Na^+; (5) 10μM Mg^{2+}; (6) 10μM Cu^{2+}; (7) 10μM Fe^{2+}; (8) 10μM Fe^{3+}.(C)Selectivity test for ROS against NO (1) 500 nM NO; (2) 10 μM HNO; (3) 10 μM $^1O_2$; (4) 10 μM NO_2^-; (5) 10 μM ClO^-; (6) 10 μM •OH; (7) 10 μM $ONOO^-$; (8) 50 μM O_2; (9) 10 μM ROO^-; (10) 10 μM $O_2^{\bullet-}$; (11) 1 μM H_2O_2. (D) Selectivity tests for amino acids against NO (1) 500 nM NO; (2) 10 μM Gln; (3) 10 μM Iso; (4) 10 μM Val; (5) 10 μM Met; (6) 10 μM Lys; (7) 10 μM L-Arg; (8) 10 μM His; (9) 10 μM D-Try; (10) 10 μM Cys; (11) 10 μM Ser; (12) 10 μM Thr; (13) 10 μM Gly; (14) 10 μM Asp; (15) 10 μM Leu.

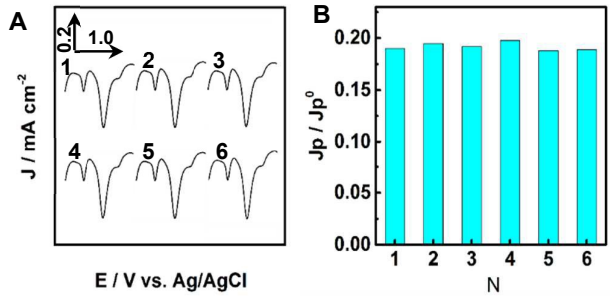

Fig. 5. (A) Reproducibility test for CNF/hemin/Nafion electrode monitored over 6 different sensors (from 1 to 6) with the addition of 300 nM NO and 50 μM O_2 in aCSF (pH 7.4). (B) The J_p/J_p^0 values taken from Fig.7A (1 to 6) of 6 sensors.

View Article Online
DOI: 10.1039/C7AN00138J

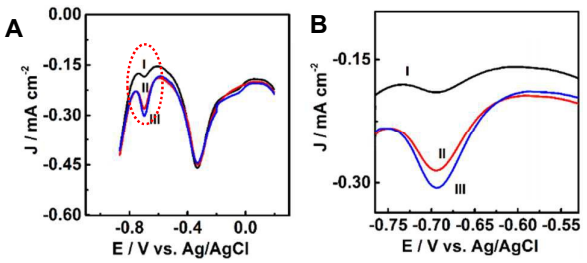

Fig. 6. (A) DPVs obtained at CNF/hemin/Nafion microelectrode in the hippocampus of normal rat brain (I) before and after (II) ischemia for 15 min, (III) after microinjection of 10 mM L-Arg into rat brain for 20 min. (B) Enlarged image of the red zone in Figure 6A.

interferences include amino acids, metal ions, neurotransmitters, reactive oxygen species (ROS), and other biological molecules, which may coexist in the brain system. As shown in Fig. 4, no obvious currents (< 6%) were obtained for cathodic peak located at -0.33 V upon the addition of amino acids, metal ions, and potential interferences. Particularly for H_2O_2, and O_2, small interference current (< 5%) was obtained at CNF/hemin/Nafion against NO signal. All results demonstrated that the present sensor possesses high selectivity for NO. Secondly, stability are also very essential for further application in complex biological system. For stability test, the present CNF/hemin/Nafion microelectrode was evaluated by performing 1000 cycles of successive cyclic voltammetric measurements in aCSF (pH 7.4). The relative standard deviation (RSD) of the peak currents obtained at CNF/hemin/Nafion changed not exceed 1.0% (Fig. S5A, SI). On the other hand, for the storing stability test, the peak current showed only 9 % current decreasing after having been stored at 4 ˚C for two weeks (Fig. S5B, SI). These results indicated that the modified electrode possesses good long-term stability. Such excellent stability of the present electrochemical sensor should thank to π-π stacking interactions between hemin and carbon nanotube fiber.

In addition, the reproducibility of CNF/hemin/Nafion microelectrode was evaluated by comparison of J_p/J_p^0 from 6 independent electrodes prepared with same method. As demonstrated in Fig. 5, the deviation of the current responses of 6 sensors prepared did not exceed 4.0% (RSD), suggesting that the CNF/hemin/Nafion possesses excellent reproducibility.

In vivo monitoring of NO in rat brain followed by cerebral ischemia

The developed ratiometric biosensor for NO detection with remarkable analytical performance, along with unique properties of CNF including miniaturization, easy to insert in the brain, and good biocompatibility, provided a facile and reliable in vivo platform for assaying NO in the live rat brain. Typical DPV responses of CNF/hemin/Nafion electrodes implanted in the hippocampus of rat brain, were obtained in the normal rat brain and rat brain followed by cerebral ischemia. As shown in Fig. 6, two cathodic peaks were clearly obtained at –0.35 V, and -0.69 V at CNF/hemin/Nafion electrode in the rat brain (Fig. 6, Curve I), which are ascribed to the reduction peak of hemin, and NO, respectively. According to the calibration, the basal levels of NO was estimated to be 61 ± 23 nM in hippocampus. The slightly potential shift possibly resulted from the shifting of an outer reference in the complicated brain environment, but our ratiometric biosensor can also effectively eliminate the shifting of outer reference through taking the peak potential of hemin as inner reference. The anodic peak current density increased to 141 ± 18 nM after ischemia for 15 min. To further verify increased current density originating from reduction of NO on the electrode surface, 10 mM Arg, NO precursor,[41, 42] was microinjected into the brain because it can be decomposed and release NO via reacting with nitric oxide synthases. As anticipated, the reduction peak current density of NO further increased by 30% after microinjection of Arg for 20 min (Fig. 6B). As a control, pure aCSF (pH 7.4) was microinjected into the brain for 15 min. However, the infusion of aCSF gave rise to slight decrease of NO electroreduction current (< 5%) (Fig. S6, SI). Therefore, it can be concluded that the increased cathodic current at -0.69 V observed in Curve II is attributed to the reduction of NO induced by cerebral ischemia. Those results further demonstrated that the present CNF/hemin/Nafion can effectively monitor NO change in brain.

Experimental

Reagents and chemicals

Hemin, dimethyl sulfoxide (DMSO), and NaClO were purchased from Aladdin-Reagent Company (Shanghai, China). Ascorbic Acid (AA), dopamine (DA), 5-hydroxytryptamine (5-HT), 5-hydroxyindoleacetic acid (5-HIAA), dihydroxy-phenyl acetic acid (DOPAC), uric acid (UA), potassium superoxide (KO_2), Nafion, H_2O_2 (30%) were purchased from Sigma-Aldrich (USA). Na_2HPO_4, NaH_2PO_4, NaOH, H_2SO_4 and other chemicals were obtained from Sinopharm Chemical Reagent Co. Ltd (China). In the selectivity experiment, superoxide anion ($O_2^{\bullet-}$) was obtained in dissolved KO_2 (150 μM) in the DMSO solution. $^1O_2$ (singlet oxygen) was generated from 3, 3'-(naphthalene-1, 4-diyl) dipropionic acid. Hydroxyl radical (•OH) was generated by Fenton reaction, which ferrous chloride was added in the presence of 10 equiv of H_2O_2. The concentration of •OH was considered to be equal to the Fe (II) concentration. Peroxynitrite (ONOO-) solution was synthesized by a mixture of sodium nitrite (0.60 M) and H_2O_2 (0.7 M) was acidified using HCl (0.6 M), and NaOH (1.5 M) was added immediately to make the solution alkaline. The excess H_2O_2 was removed by passing the solution through a short column of manganese dioxide. L-arginine (Arg), L-cysteine (Cys), L-glutamine (Glu), glycine (Gly), L-histidine (His), L-isoleucine (Iso), L-leucine (Leu), L-lysine (Lys), L-methionine (Met), L-phenylalanine (Phe), L-serine (Ser), L-threonine (Thr), L-valine (Val) were purchased from J&K Scientific (Beijing, China). DL-lactic acid, L-tyrosine,

View Article Online
DOI: 10.1039/C7AN00138J

and tyramine were obtained from Tokyo Chemical Industry (TCI) (Japan).

Artificial cerebrospinal fluid (aCSF) was prepared by mixing $CaCl_2$ (1.1 mM), NaCl (126 mM), KCl (2.4 mM), $NaHCO_3$ (27.5 mM), KH_2PO_4 (0.5 mM), $MgCl_2$ (0.85 mM), and Na_2SO_4 (0.5 mM) into doubly distilled water, and the pH of mixed solution was adjusted to 7.4. All reagents and chemicals were analytical grade and used directly without further purification. Double-distilled water used in all experiments was obtained from a Millipore water purification system (Milli-Q, ⩾18.2 MΩ•cm).

Above all, NO solution was prepared by adding NO precursor, diethylamine NONOate sodium salt, into 10 mM NaOH solution followed by dilution with aCSF(pH 7.4), according to a protocol developed in previous literature about NO detection.[43] All solutions were pre-bubbled with N_2 for 20 min to remove the dissolved oxygen unless otherwise stated, and stored at 4 ˚C.

Apparatus and Instruments.

Electrochemical experiment was performed on an electrochemical working station (CHI 660D, Shanghai, China) in aCSF buffer solution (pH 7.4). A three-electrode system, with an Ag/AgCl (KCl-saturated) electrode as the reference electrode, and a platinum wire as the counter electrode, and various modified microelectrodes as working electrode. All potentials mentioned hereafter are versus Ag/AgCl (KCl-saturated) electrode. All electrochemical experiments were carried out at 25 ˚C. The differential pulse voltammetry (potential step, 4 mV; modulation amplitude, 50 mV; pulse width, 0.05 s; pulse period, 0.5 s) was used to detect NO. X-ray photoelectron spectroscopy (XPS, AXIS Ultra DLD, Japan) equipped with an Al K_α (1486.6 eV photons) was used to characterize the nanocomposites. The scanning electron microscopy (SEM) images were obtained on a Hitachi S4800 field emission scanning electron microscope. The transmission electron microscopy (TEM) images were acquired by High Resolution Transmission Electron Microscopy (HRTEM, JEOL JEM- 2010F, 200kV). Ultraviolet-Visible spectra (UV-Vis) were performed on UV-Vis spectrophotometer (UH5300, Japan). The concentration of O_2 in solution was measured by Dissolved Oxygen Meters (JENCO 9173 DO, China). In this paper, error bar represents the standard deviation from three independent assays.

Synthesis of CNF.

The carbon nanotube fiber (CNF) was dry-spun from spinnable multi-walled carbon nanotube (MWCNT) arrays at a rotating rate of 2000 rpm.[44] The MWCNT arrays were synthesized by chemical vapor deposition in a quartz tube furnace with a diameter of 2 inch. In a typical synthesis, Fe (1 nm) and Al_2O_3 (10 nm) were sequentially deposited on a silicon substrate by electron beam evaporation and used as the catalyst. Ethylene with a flowing rate of 90 sccm was used as carbon source, and a mixture of Ar (400 sccm) and H_2 (30 sccm) was used as carrying gas. Then, the CNF was put in pipe furnace under 600 ˚C for 2h in the atmosphere of N_2 gas to activate and clean the surface of MWCNT. The area of CNF was estimated according its geometrical area according to the following equation: $A_{CNF} = 2\pi rl+2\pi r$, in which r is the radius of CNF, l is the length of carbon nanotube fiber exposed outside of glass capillary tip.

The fabrication of microelectrode.

A single CNF was attached to a copper wire with silver conducting paste. Then, the CNF attached copper wire was carefully inserted into the capillary with CNF exposed to the fine open end of the capillary and Cu wire exposed to the other end of the capillary. Both open ends of the capillary were sealed with epoxy resin with 1:1 ethylendiamine as the harder and the excess epoxy on the fiber was carefully removed with acetone. After that, CNF microelectrode was dried at 60 ºC for overnight. The exposed carbon fiber was cut to ~500 μm in length under a microscopy. Prior to modification, the fabricated CFME was first sequentially sonicated in acetone, 3.0 M HNO_3, 1.0 M KOH, and Milli-Q each for 2 min. Then, CNF microelectrode was immerged into the DMSO solution of 10 mM hemin. The obtained microelectrode was denoted as CNF/hemin electrode. Then, the CNF/hemin electrode was dipped into 5% w/v Nafion ethanol solution and allowed the solvent to dry in the air, which was denoted as CNF/hemin/Nafion.

In vivo measurements.

The adult male Wistar rats (250-300 g, the age at the time of 3-4 months) for in vivo measurement were purchased from Shanghai SLAC Laboratory Animal Co. Ltd (Shanghai, China). All procedures for animals were performed with approval of Animal Ethics Committee in East China Normal University. Rats were anesthetized with Chloral hydrate (300 mg/kg, i.p.). Additional doses of 100 mg/kg (i.p.) was used to remain anesthesia after each hour. Then, the rats were placed in a stereotaxic frame (Beijing Tide-Gene Biotechnology Development Center) with the incisor bar set at 5 mm above the interaural line. Two holes were drilled with cranial drill on rat's skull. The CNF/hemin/Nafion microelectrode was implanted in hippocampus of rat brain (AP = 5.0 mm, L = 5.0 mm from bregma, V = 2.5 mm from the surface of the skull). Another 2 mm plastical cannula was located at ~5 mm far from working electrode, in which reference and counter electrodes were introduced. During the whole experiment, the rat's body temperature was remained at 37 ˚C with a heating pad and supplements of chloral hydrate were given as required.

In the two vessel occlusion ischemia models, the bilateral common carotids arteries were ligated as reported previously. Briefly, the bilateral common carotid arteries were first separated via a ventral middle line cervical incision. Then, the atlantooccipital membrane was exposed from the left side by retraction of the trachea and esophagus to the right. A vascular clip stainless steel was used to make the basilar artery occluded. Blood flow in the basilar, after the cessation, could be visually confirmed. Occultation in both common carotid arteries was carried out using two Yasargil miniclips. Ischemic duration was timed as soon as the last clip was used to the

View Article Online
DOI: 10.1039/C7AN00138J

common carotid artery and the whole ischemic procedure usually lasted for about 15 min.

Conclusions

In summary, through synthesizing CNF and employing hemin as selective catalyst and inner reference element, we have developed a facile strategy for ratiometric detection of NO. The present biosensor demonstrated high accuracy and stability, as well as high selectivity against metal ions, neurotransmitters, amino acid, and ROS/RNS. The developed method with theoretical simplicity, and less instrumental demands, has been successfully applied for reliable detection of NO in the rat brain followed by cerebral ischemia. Additionally, the present study has provided a method for designing and constructing more reliable ratiometric approach for other important biological species which are related to brain chemistry.

Acknowledgements

The authors greatly appreciate the financial support from NSFC for distinguished Yong Scholars (21325521 for Y. T. and 21625502 for Z. D.) and NSFC (21475062 for Z. D, 21635003 for Y. T., 21305104, 21545002, and 21675054 for L. Z.). Partially Supported by Open Funding Project of the State Key Laboratory of Bioreactor Engineering. The authors thank Dr. Xuemei Sun and Prof. Huisheng Peng at Fudan University for providing the CNF.

Notes and references

1. C. Nathan and Q.-w. Xie, *Cell*, 1994, **78**, 915-918.
2. T. V. Bliss and G. L. Collingridge, *Nature*, 1993, **361**, 31.
3. R. G. Knowles and S. Moncada, *Trends Biochem. Sci*, 1992, **17**, 399-402.
4. Z. Taha, F. Kiechle and T. Malinski, *Biochem. Biophys. Res. Commun.*, 1992, **188**, 734-739.
5. N. S. Bryan and M. B. Grisham, *Free Radical Biol. Med.*, 2007, **43**, 645-657.
6. L. Baumane, M. Dzintare, L. Zvejniece, D. Meirena, L. Lauberte, V. Sile, I. Kalvinsh and N. Sjakste, *Acta anaesthesiologica scandinavica*, 2002, **46**, 378-383.
7. M. Feelisch and J. Stamler, *Methods in nitric oxide research*, Wiley-Blackwell, 1996.
8. J. Cui, K. Hu, J.-J. Sun, L.-L. Qu and D.-W. Li, *Biosens. Bioelectron.*, 2016, **85**, 324-330.
9. T. Nagano and T. Yoshimura, *Chem. Rev.*, 2002, **102**, 1235-1270.
10. M. H. Lim, B. A. Wong, W. H. Pitcock, D. Mokshagundam, M.-H. Baik and S. J. Lippard, *J. Am. Chem. Soc.*, 2006, **128**, 14364-14373.
11. M. N. Friedemann, S. W. Robinson and G. A. Gerhardt, *Anal. Chem.*, 1996, **68**, 2621-2628.
12. R. M. Santos, M. S. Rodrigues, J. Laranjinha and R. M. Barbosa, *Biosens. Bioelectron.*, 2013, **44**, 152-159.
13. F. X. Hu, J. Le Xie, S. J. Bao, L. Yu and C. M. Li, *Biosens. Bioelectron.*, 2015, **70**, 310-317.
14. L. Wang, P. Hu, X. Deng, F. Wang and Z. Chen, *Biosens. Bioelectron.*, 2013, **50**, 57-61.
15. B. J. Privett, J. H. Shin and M. H. Schoenfisch, *Chem. Soc. Rev.*, 2010, **39**, 1925-1935.
16. S.-K. Kang, R. K. Murphy, S.-W. Hwang, S. M. Lee, D. V. Harburg, N. A. Krueger, J. Shin, P. Gamble, H. Cheng and S. Yu, *Nature*, 2016, **530,** 71-76.
17. H. Cheng, X. Wang and H. Wei, *Anal. Chem.*, 2015, **87**, 8889-8895.
18. M. Zhang, P. Yu and L. Mao, *Acc. Chem. Res.*, 2012, **45**, 533-543.
19. A. Karajić, S. Reculusa, S. Ravaine, N. Mano and A. Kuhn, *ChemElectroChem*, 2016, **3**, 2031-2035.
20. S. Shiba, K. Yoshioka, D. Kato, S. Ishihara, H. Anzai, N. Saito and O. Niwa, *J. Electroanal. Chem.*, 2016, **779**, 86-91.
21. W. Harreither, R. l. Trouillon, P. Poulin, W. Neri, A. G. Ewing and G. Safina, *Anal. Chem.*, 2013, **85**, 7447-7453.
22. X. Liu, M. Zhang, T. Xiao, J. Hao, R. Li, L. Mao. *Anal. Chem.* 2016, **88,** 7238-7244.
23. Y. Luo, L. Zhang, W. Liu, Y. Yu and Y. Tian, *Angew. Chem.*, 2015, **127**, 14259-14262.
24. J. Zhou, C. Liao, L. Zhang, Q. Wang and Y. Tian, *Anal. Chem.*, 2014, **86**, 4395-4401.
25. L. Zhang, Y. Han, F. Zhao, G. Shi and Y. Tian, *Anal. Chem.*, 2015, **87**, 2931-2936.
26. A. Zamora-Gálvez, A. Ait-Lahcen, L. A. Mercante, E. Morales-Narváez, A. Amine and A. Merkoçi, *Anal. Chem.*, 2016, **88**, 3578-3584.
27. F. O. Brown, N. J. Finnerty and J. P. Lowry, *Analyst*, 2009, **134**, 2012-2020.
28. S. Griveau, C. Dumézy, J. Séguin, G. G. Chabot, D. Scherman and F. Bedioui, *Anal. Chem.*, 2007, **79**, 1030-1033.
29. L. Xiang, P. Yu, M. Zhang, J. Hao, Y. Wang, L. Zhu, L. Dai, L. Mao. *Anal. Chem.* 2014, **86,** 5017-5023..
30. F. Zhao, L. Zhang, A. Zhu, G. Shi and Y. Tian, *Chem. Commun.*, 2016, **52**, 3717-3720.
31. H. Li, N. y. Arroyo-Currás, D. Kang, F. Ricci and K. W. Plaxco, *J. Am. Chem. Soc.*, 2016, **138**, 15809-15812.
32. H. Chen, C. Jiang, C. Yu, S. Zhang, B. Liu and J. Kong, *Biosens. Bioelectron.*, 2009, **24**, 3399-3411.
33. A. Ledo, R. M. Barbosa, G. A. Gerhardt, E. Cadenas and J. Laranjinha, *Proc. Nat. Acad. Sci. U. S. A.*, 2005, **102**, 17483-17488.
34. L. Shang, X. Liu, J. Zhong, C. Fan, I. Suzuki and G. Li, *Chem. Lett.*, 2003, **32**, 296-297.
35. F. Bedioui, S. Trevin, V. Albin, M. Guadalupe, G. Villegas and J. Devynck, *Anal. Chim. Acta*, 1997, **341**, 177-185.
36. Z. Zhang, K. Guo, Y. Li, X. Li, G. Guan, H. Li, Y. Luo, F. Zhao, Q. Zhang and B. Wei, *Nat. Photonics*, 2015, **9**, 233-238.
37. Y. Xu, L. Zhao, H. Bai, W. Hong, C. Li and G. Shi, *J. Am. Chem. Soc.*, 2009, **131**, 13490-13497.
38. D. L. Compton and J. A. Laszlo, *J. Electroanal. Chem.*, 2002, **520**, 71-78.
39. J. Chen, U. Wollenberger, F. Lisdat, B. Ge and F. W. Scheller, *Sens. Actu. B: Chem.*, 2000, **70**, 115-120.
40. M. T. de Groot, M. Merkx, A. H. Wonders and M. T. Koper, *J. Am. Chem. Soc.*, 2005, 127, 7579-7586.
41. R. M. Palmer, D. Ashton and S. Moncada, *Nature*, 1988, **333**, 664-666.
42. L. J. Ignarro, *Nitric oxide: biology and pathobiology*, Academic press, 2000.
43. H. Li, M. Yu, F. Wang, P. Liu, Y. Liang, J. Xiao, C. Wang, Y. Tong and G. Yang, *Nat. Commun.*, 2013, **4**, 1894.

View Article Online
DOI: 10.1039/C7AN00138J

44. T. Chen, Z. Cai, Z. Yang, L. Li, X. Sun, T. Huang, A. Yu, H. G. Kia and H. Peng, *Adv. Mater.*, 2011, **23**, 4620-4625.